Chemical Science

ROYAL SOCIETY OF CHEMISTRY

EDGE ARTICLE

View Article Online
View Journal | View Issue

Cite this: *Chem. Sci.*, 2024, **15**, 6583

All publication charges for this article have been paid for by the Royal Society of Chemistry

Fine-regulation of gradient gate-opening in nanoporous crystals for sieving separation of ternary C3 hydrocarbons†

Shuang Liu,‡[a] Yuhang Huang,‡[b] Jingmeng Wan,[b] Jia-Jia Zheng,[c] Rajamani Krishna,[d] Yi Li,[b] Kai Ge,*[b] Jie Tang[b] and Jingui Duan *[b]

The adsorptive separation of ternary propyne (C_3H_4)/propylene (C_3H_6)/propane (C_3H_8) mixtures is of significant importance due to its energy efficiency. However, achieving this process using an adsorbent has not yet been accomplished. To tackle such a challenge, herein, we present a novel approach of fine-regulation of the gradient of gate-opening in soft nanoporous crystals. Through node substitution, an exclusive gate-opening to C_3H_4 (17.1 kPa) in **NTU-65-FeZr** has been tailored into a sequential response of C_3H_4 (1.6 kPa), C_3H_6 (19.4 kPa), and finally C_3H_8 (57.2 kPa) in **NTU-65-CoTi**, of which the gradient framework changes have been validated by *in situ* powder X-ray diffractions and modeling calculations. Such a significant breakthrough enables **NTU-65-CoTi** to sieve the ternary mixtures of $C_3H_4/C_3H_6/C_3H_8$ under ambient conditions, particularly, highly pure C_3H_8 (99.9%) and C_3H_6 (99.5%) can be obtained from the vacuum PSA scheme. In addition, the fully reversible structural change ensures no loss in performance during the cycling dynamic separations. Moving forward, regulating gradient gate-opening can be conveniently extended to other families of soft nanoporous crystals, making it a powerful tool to optimize these materials for more complex applications.

Received 16th October 2023
Accepted 17th March 2024

DOI: 10.1039/d3sc05489f

rsc.li/chemical-science

Introduction

Efficient separation of the ternary C3 hydrocarbons is crucial for the petrochemical industry as C_3H_6 is an essential feedstock for valuable commodities.[1] Currently, the separation process involves energy-intensive catalytic hydrogenation and cryogenic distillation, which accounts for nearly 3% of all separation energy.[1–3] Therefore, there is a need for a more energy-efficient technology for this task. Adsorption separation using porous materials, specifically porous coordination polymers (PCPs), shows great promise due to their finely designed pore chemistry.[4–13] In this regard, recent progress has been made in binary separations using strategies such as π-complexation, sieving strategies and kinetic diffusion.[14–23] However, the similar molecular sizes and kinetic diameters exacerbate the challenge of $C_3H_4/C_3H_6/C_3H_8$ separation, particularly by one material.

Recent research has shown that the purification of ethylene from a complex mixture of C2 hydrocarbons and carbon dioxide can be achieved using sequentially packed sorbents, where the three impurities were captured by three PCPs.[24] Although this strategy requires overcoming the difficulties of preparation of the three materials, and also their rational packing, it enables us to believe that integrating gradient sorbent–sorbate interactions may address the challenge of $C_3H_4/C_3H_6/C_3H_8$ separation in a single domain, as well as the precise understanding of hierarchical sites or gradient gate-openings.

The concept of hierarchical sites holds certain theoretical feasibility, but its implementation is hindered by the significant limitations in rational assembly of these sites in a confined nanospace. Comparably, the strategy of gradient gate-openings shows promising prospects. Since the early reports of soft crystals,[25,26] the soft nature of these materials has been gradually understood, that is, the stronger the interaction, the earlier the gate-opening.[27,28] In addition, soft frameworks can exhibit sensitive responses to even extremely small stimuli.[29–31] Given these advantages, significant efforts have been dedicated to the construction of soft PCPs;[27,29,32–35] however, neither the fine predesign nor function-oriented synthesis of such a material,

[a]*Henan Engineering Research Center for Green Synthesis of Pharmaceuticals, College of Chemistry and Chemical Engineering, Shangqiu Normal University, Shangqiu 476000, China*

[b]*State Key Laboratory of Materials-Oriented Chemical Engineering, College of Chemical Engineering, Nanjing Tech University, Nanjing 211816, China. E-mail: gekai@njtech.edu.cn; duanjingui@njtech.edu.cn*

[c]*Laboratory of Theoretical and Computational Nanoscience, National Center for Nanoscience and Technology, Chinese Academy of Sciences, Beijing 100190, China*

[d]*Van't Hoff Institute for Molecular Sciences, University of Amsterdam, Science Park 904, 1098 XH Amsterdam, The Netherlands*

† Electronic supplementary information (ESI) available. CCDC 2284815–2284818. For ESI and crystallographic data in CIF or other electronic format see DOI: https://doi.org/10.1039/d3sc05489f

‡ These authors contributed equally to this work.

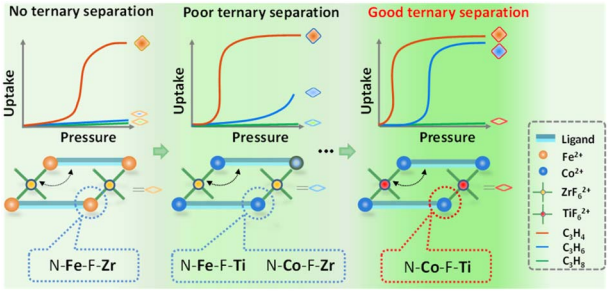

Scheme 1 Illustration of fine-regulation of gradient gate-opening in soft **NTU-65-series** *via* node substitution for sieving separation of C3 hydrocarbons in a single domain.

whose framework can sequentially recognize these similar molecules, has yet been reported.

During our investigation of porous materials,[20,36,37] we have reported a soft crystal, **NTU-65**, $[Cu(\mathbf{L})_2(SiF_6)]$ (**L** = 1,4-di(1*H*-imidazolyl)benzene). The temperature dependent gate-opening allows it to show a sieving separation of $C_2H_4/C_2H_2/CO_2$ mixtures.

However, this framework cannot separate the equimolar C_3H_6/C_3H_8 due to a small difference in uptake at this ratio caused by the gate-opening effect which either occurs too early or too late (Fig. S2†). Inspired by reticular chemistry[38] and **NTU-65**, herein, we report a fine tuning of the framework softness *via* node substitution in a series of PCPs (**NTU-65-series**: **NTU-65-FeZr**, **NTU-65-FeTi**, **NTU-65-CoZr** and **NTU-65-CoTi**, Scheme 1), as the metal nodes may alter the transformation characteristics of soft structures. As expected, a sole gate-opening toward C_3H_4 in **NTU-65-FeZr** evolves into a gradient response to C_3H_4 and C_3H_6 in **NTU-65-CoTi**, yielding an unprecedented breakthrough of sieving separation of $C_3H_4/C_3H_6/C_3H_8$.

Results and discussion

Solvothermal reactions of **L** and the corresponding metal salt provide **NTU-65-series** (Fig. S3†). They crystallize in the monoclinic system (Table S1†) and adopt the same coordination configurations. The M1 centres (M1: Fe^{2+} or Co^{2+}) of **NTU-65-series** are connected by four imidazole N atoms in a planar configuration from four **L** and two F atoms in the axial vertex from two $M_2F_6^{2-}$ (M_2: Zr^{4+} or Ti^{4+}) ions. As a result, cross-linked 2D channels are observed in the packed frameworks, although the window apertures undergo minimal changes (Fig. 1a, b and S4–S8†), along with similar accessible volumes (43.5%, 44.8%, 42.4% and 44.8%).[39] To reach the adjacent nodes, the dihedral angle between the benzene and imidazole rings in **L** in **NTU-65-series** shows significant changes. For example, the angle of the $\mathbf{L}_{Cis}$ in **NTU-65-FeZr** is as large as 14.81°, while this angle decreases to 3.45° in **NTU-65-FeTi** (Fig. 1c). Additionally, the dihedral angle in $\mathbf{L}_{Trans}$ in **NTU-65-CoTi** is up to 22.69°. Therefore, different degrees of softness are expected in the **NTU-65-series**. Phase purity of the four crystals has been confirmed by X-ray powder diffraction measurement (Fig. S9†). In addition, all samples are thermally stable, up to 350 °C (Fig. S10†).

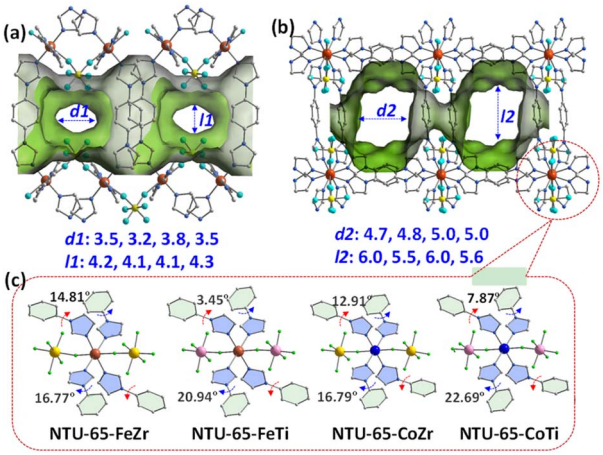

Fig. 1 Crystal structure of **NTU-65-series** along the *a*-axis (a) and *b*-axis (b). Comparison of the dihedral angle in **L** in **NTU-65 series** (c).

Permanent porosity of the activated **NTU-65-series** was evaluated using N_2 adsorption measurements at 77 K (Fig. S12†). Initially, all samples show minimal N_2 uptake until reaching P/P_0 = 0.61, 0.26, 0.27 and 0.24. However, a peculiar 'kink' phenomenon occurred in all of them. This is due to the rapid increase in adsorption capacity of the crystals after instantaneous gate-opening under this condition, accompanied by a rapid decrease in system pressure, to P/P_0 = 0.10, 0.07, 0.05 and 0.04, respectively. Subsequently, N_2 uptake increases with increased pressure in **NTU-65-FeZr**, while type-I adsorption isotherms were observed in **NTU-65-FeTi** and **NTU-65-CoTi**. Differently, **NTU-65-CoZr** exhibits a second adsorption platform before reaching P/P_0 = 0.6, followed by pressure-dependent uptake. Despite these differences, all four crystals demonstrated a similar maximum N_2 capacity (219.5 to 236.2 $cm^3\ g^{-1}$). Evaluated by using these isotherms, the crystals exhibit comparable surface areas (540–610 $m^2\ g^{-1}$) and pore volumes (0.34–0.36 $cm^3\ g^{-1}$) (Fig. S13, S14 and Table S2†). Additionally, all isotherms display desorption hysteresis, confirming the filling effect of the soft frameworks.[40,41]

To further investigate structural softness, CO_2 isotherms were collected at 195 K, as CO_2 may interact differently with the frameworks compared to N_2.[42,43] Unlike the 'kink' phenomenon in the above N_2 isotherms, all CO_2 uptakes of the **NTU-65-series** increase with elevated pressure. Meanwhile, gradient adsorption platforms indicating sequential gate-openings were clearly observed in **NTU-65-series**. For **NTU-65-FeZr**, the first gate-opening occurs at 2.1 kPa, followed by the second and third gate-opening at 22.8 and 56.3 kPa, respectively (Fig. 2a). However, **NTU-65-FeTi** shows an earlier first gate-opening pressure (**OP**) of 1.7 kPa. The second and third gate-openings in **NTU-65-FeZr** merge into one in **NTU-65-FeTi**, at 31.4 kPa (Fig. 2b). Notably, three gate-openings appear again in **NTU-65-CoZr** (starting at 0.8, 14.6 and 45.8 kPa), whose responsive pressures are all lower than that of **NTU-65-FeZr**, and the first **OP** is also lower than that of **NTU-65-FeTi** (Fig. 2c). Remarkably, **NTU-65-CoTi** exhibits an advancement of the first **OP** at 0.5 kPa, followed by a second quick uptake at 18.8 kPa (Fig. 2d). Therefore, these isotherms

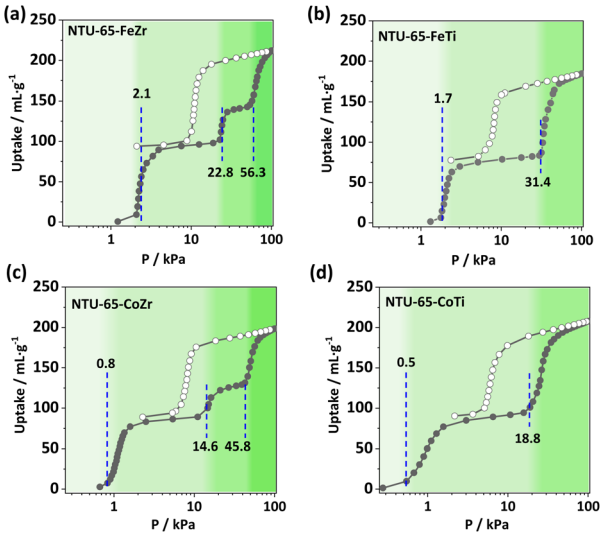

Fig. 2 CO_2 adsorption isotherms of NTU-65-series (a)–(d) at 195 K.

indicate that the four activated crystals possess non-porous characteristics and can be opened by N_2 or CO_2 once the stimuli exceed the energy barrier controlling the framework closure. Meanwhile, the gradually decreased pressure (2.1 to 0.5 kPa) for the first gate-opening reflects the fact that the four frameworks show different sensitivities to external stimuli. Additionally, the difference in multi-step gate-openings in them validates the effectiveness of the node substitution strategy in regulation of the framework with gradient softness, which may provide a promising platform for sequential recognition of gases with extremely small differences.

To investigate the function of gradient and sensitive gate-openings, adsorption isotherms of C_3H_4, C_3H_6 and C_3H_8 were collected on **NTU-65-series** (Fig. 3 and S15–S18†). **NTU-65-FeZr** exhibits minimal uptake of C_3H_6 and C_3H_8 at the threshold pressure, whereas C_3H_4 adsorption begins at 17.1 kPa with a maximum capacity of 74.7 $cm^3\ g^{-1}$ (Fig. 3a). Meanwhile, the starting **OP** is advanced to 10.0 kPa in **NTU-65-FeTi**, along with nearly the same C_3H_4 capacity (69.0 $cm^3\ g^{-1}$) (Fig. 3b). Unlike **NTU-65-FeZr**, C_3H_6 molecules open the framework of **NTU-65-FeTi** at 66.0 kPa with a capacity of 44.2 $cm^3\ g^{-1}$ at 100 kPa (Fig. 3c). Interestingly, the **OP** of the three gases (C_3H_4: 5.3 kPa, C_3H_6: 46.2 kPa and C_3H_8: 66.8 kPa) exhibit a forward movement again in **NTU-65-CoZr** (Fig. 3d). However, the isotherms indicate two crucial issues that may arise during the dynamic separation of such ternary mixtures: (1) insufficient partial pressure for C_3H_4 adsorption (far larger than 1 kPa); and (2) lower separation performance between C_3H_6 and C_3H_8 (small uptake difference of only 7.6 $cm^3\ g^{-1}$ at around 50 kPa). Remarkably, these issues may be solved by using **NTU-65-CoTi**, which exhibits rapid uptake of C_3H_4 at 1.6 kPa and a significantly improved uptake difference between C_3H_6 and C_3H_8, reaching as high as 55.9 $cm^3\ g^{-1}$ at 50 kPa. Additionally, the total C_3H_4 capacity is increased to 95.9 $cm^3\ g^{-1}$. Moreover, the uptake ratios of binary mixtures (C_3H_4/C_3H_6, C_3H_6/C_3H_8 and C_3H_4/C_3H_8) were significantly and simultaneously improved compared to that of other benchmark materials (Table 1 and S3†).

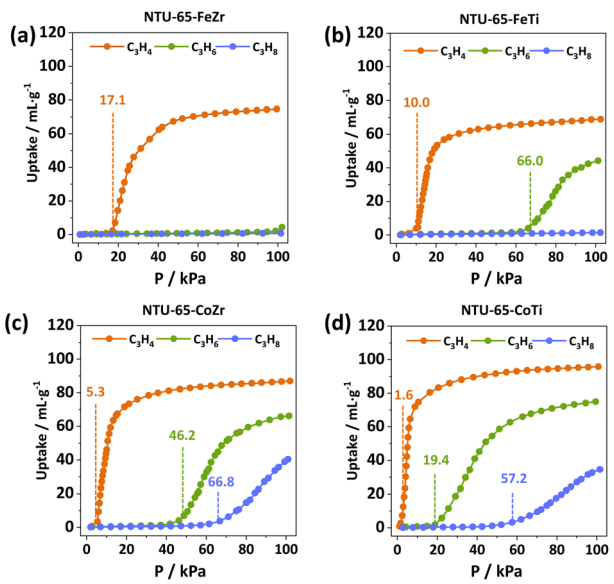

Fig. 3 C_3H_4, C_3H_6 and C_3H_8 adsorption isotherms of NTU-65-series (a)–(d) at 273 K.

To confirm the systemic structural changes, *in situ* powder X-ray diffraction patterns/sorption measurements were performed (Fig. 4). The characteristic peaks corresponding to crystal faces of [0 2 0] and [0 0 1] in the as-synthesized phases (at about 6.5 and 7.2°) become weaker and shift to a higher-angle region in the activated crystals, indicative of structural contraction commonly observed in flexible PCPs. However, these two peaks reappear at similar positions to those obtained from their as-synthesized phases after an increase in pressure. Additionally, these open structures transform back into the closed state when the pressure decreases to a very low value, showing reversible sorption and structural changes in **NTU-65-series**. In addition, gas-loaded crystallographic analysis has also been attempted to explore the detailed structural changes. However, the small crystal size and crack after activation results in extremely weak or no diffraction. To understand the trend in softness of these PCPs, we conducted density functional theory (DFT) calculations taking C_3H_4 as the probe molecule (Fig. S20†). Previously, we have shown that the gate-opening pressure of PCPs induced by gas adsorption is dependent on the binding energy of the gas molecule with the PCP.[44] We therefore calculated the binding energies of C_3H_4 with the **NTU-65-series**. The binding energy increases (becomes more negative) in the following order: **NTU-65-FeZr** (−7.8 kcal mol^{-1}) < **NTU-65-FeTi** (−8.1 kcal mol^{-1}) < **NTU-65-CoZr** (−8.5 kcal mol^{-1}) < **NTU-65-CoTi** (−9.1 kcal mol^{-1}). This is consistent with the order of gate-opening pressure of these PCPs in response to C_3H_4 adsorption for these PCPs (Fig. 3).

The sequential recognition of C3 hydrocarbons encouraged us to perform dynamic separations. Given the commonly encountered ratio of C3 hydrocarbons in industry, a simulated feed-gas of $C_3H_4/C_3H_6/C_3H_8$ (0.5/49.75/49.75, v/v/v) was used for breakthrough experiments at 273 K. Consistent with the single-component gas isotherms, C_3H_6 and C_3H_8 elute simultaneously

Table 1 Summarized capacities ($cm^3\ g^{-1}$) and uptake ratios of C3 hydrocarbons for **NTU-65-series** at 273 K

	C_3H_4	C_3H_6	C_3H_8	Uptake ratios		
PCPs	0.1 bar	0.5 bar	0.5 bar	C_3H_4/C_3H_6 (0.1/0.5)	C_3H_6/C_3H_8 (0.5/0.5)	C_3H_4/C_3H_8 (0.1/0.5)
NTU-65-CoTi	73.93	57.44	1.55	1.28	37.05	47.70
NTU-65-CoZr	46.24	8.55	0.96	5.41	8.91	48.17
NTU-65-FeTi	3.93	1.27	0.73	3.01	1.74	5.34
NTU-65-FeZr	0.59	0.74	0.51	0.80	1.45	1.16

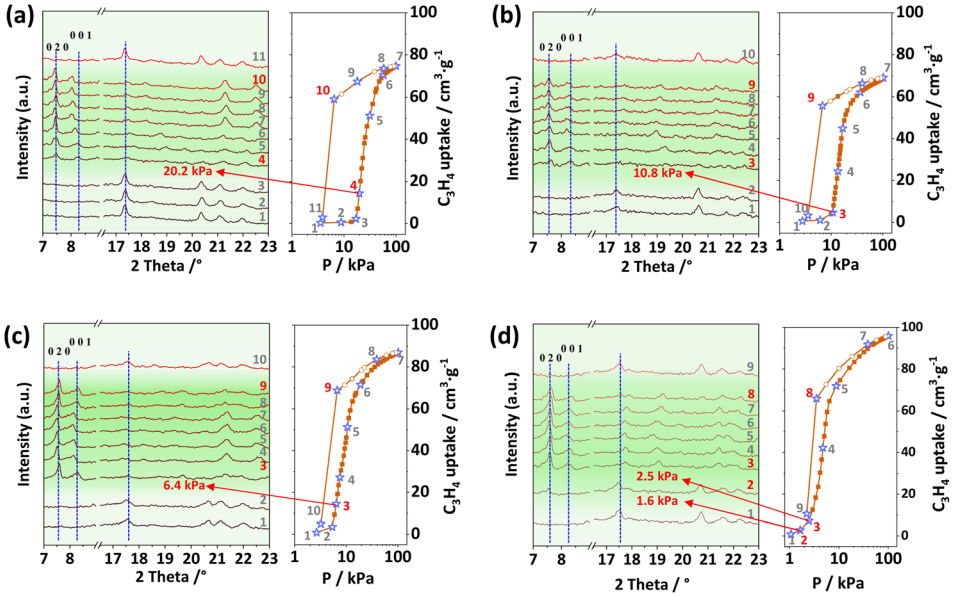

Fig. 4 *In situ* PXRD patterns of **NTU-65-FeZr** (a), **NTU-65-FeTi** (b), **NTU-65-CoZr** (c) and **NTU-65-CoTi** (d) during C_3H_4 adsorption/desorption at 273 K.

from the **NTU-65-FeZr** sample bed, while C_3H_4 was captured until 85.8 min g^{-1}, showing impossible ternary separation (Fig. 5a). For **NTU-65-CoZr**, C_3H_8 was detected as the first elution at 19.3 min g^{-1}, followed by C_3H_6 at 27.8 min g^{-1}. Additionally, C_3H_4 passes through the column at 106.3 min g^{-1} (Fig. 5b). Considering the **OP** of C_3H_6 (46.2 kPa) and the small uptake difference (7.6 $cm^3\ g^{-1}$) of C_3H_6/C_3H_8 in **NTU-65-CoZr**, the observable separation time of C_3H_6/C_3H_8 should be attributed to the slight pore opening, caused by accumulated C_3H_6 adsorption. This phenomenon is similar to the selective C_3H_4 or C_2H_2 capture in GeFSIX-dps-Zn[45] and $Co(4\text{-DPDS})_2MoO_4$,[46] respectively, where the partial pressures of C_3H_4 (10 kPa) or C_2H_2 (1 kPa) in the feed-gas for breakthrough separations are lower than that of the corresponding **OP**s (~16 kPa and ~17 kPa) of the frameworks at the same temperature. In addition, a similar and insufficient ternary separation was also observed in **NTU-65-FeTi**. Remarkably, **NTU-65-CoTi** exhibits a significant separation of the ternary mixture of $C_3H_4/C_3H_6/C_3H_8$, in which highly pure C_3H_8 elutes out at 17.0 min g^{-1}, while the outflows of C_3H_6 and C_3H_4 from the sample bed are around 41.1 min g^{-1} and 132.9 min g^{-1} (Fig. 5c). Additionally, the further extended retention time of C_3H_4 (from 85.8 min g^{-1} in **NTU-65-FeZr** to 132.9 min g^{-1} in **NTU-65-CoTi**) reflects the increased cumulative effect in **NTU-65-series**, as structural deformation becomes easier. To the best of our knowledge, the PCPs, including rigid and soft frameworks, have been widely explored for gas separations; however, this is the first example that can separate C3 hydrocarbons in one-step in a single domain. Furthermore, this promising separation was also confirmed at increased velocity (5 and 10 mL min^{-1}) of such ternary mixtures, as well as the binary mixtures (Fig. S21–S27 and Tables S4–S7†). More importantly, due to the reversible structural changes, there is almost no performance loss during the cycling measurments on **NTU-65-CoTi** (Fig. 5d and S28†), a critical factor in evaluating the feasibility of the adsorbents.

Based on these breakthrough results results, how the **NTU-65-CoTi** might be possible to procure pure C_3H_6 and C_3H_8 are mostly expected. As shown in Fig. 5e, two beds are needed, Bed A and B, both packed with **NTU-65-CoTi**.[47,48] During the adsorption cycle, the two beds A and B operate sequentially. The operation of Bed A and B should last for at least 130 min g^{-1} and 35 min g^{-1}, respectively. Highly pure C_3H_8 (99.9%, GC limitation) is recovered from Bed B at the end of the adsorption cycle. After termination of the adsorption cycle, both Bed A and B are subjected to counter-current vacuum desorption. From Bed A, the product C_3H_4 with improved concentration (from 0.5% to

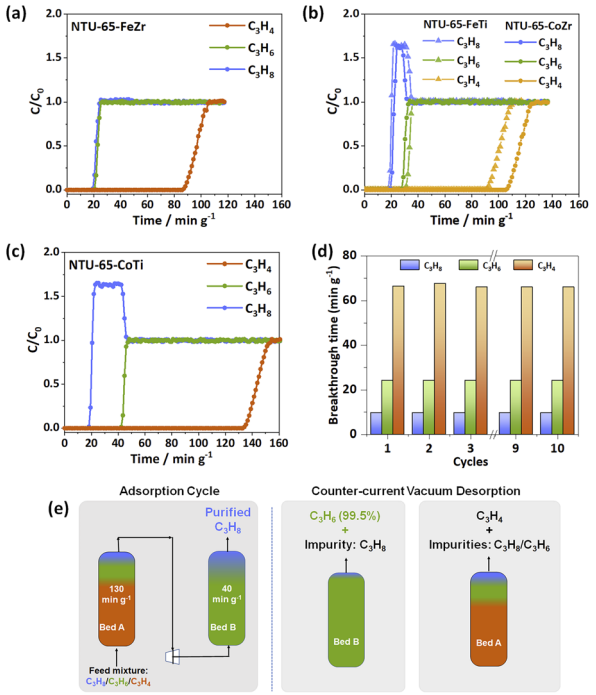

Fig. 5 Breakthrough curves of **NTU-65-series** (a)–(d) for $C_3H_4/C_3H_6/C_3H_8$ (0.5/49.75/49.75, v/v/v, 2 mL min^{-1}) at 273 K. Cycling performance of **NTU-65-CoTi** (5 mL min^{-1}) (d). Schematic representation of the separation of C3 ternary mixtures using two packed beds of **NTU-65-CoTi** in a vacuum swing adsorption process (e).

6.3%) can be obtained, while from Bed B, the product C_3H_6 can be harvested with a purity approaching 99.5%.

Conclusions

In summary, due to the demand for energy-efficient separation of C3 hydrocarbons, we here report a gradient regulation of framework softness *via* the node substitution approach. The exclusive response to C_3H_4 in **NTU-65-FeZr** has been tailored into a sequential capture of C_3H_4 and C_3H_6 in **NTU-65-CoTi**. This breakthrough enables an unprecedented ability for sieving separation of the ternary $C_3H_4/C_3H_6/C_3H_8$ mixtures in a single domain. By following designed procedures, highly pure C_3H_8 (99.9%) and C_3H_6 (99.5%) can be obtained. Moving forward, given that the conditions for feasible gas separation vary significantly, the precise understanding and ability to tune the gate-openings of soft PCPs are particularly important, potentially indicating a path to other challenging multi-component systems.

Data availability

The data supporting the findings of this study are available within the article and/or its ESI.†

Author contributions

J. D. conceived the research idea and designed the experiments. S. L. and Y. H. conducted the experiments. S. L., Y. H., J. W., Y. L., and J. T. analysed and discussed the data. J. Z. and K. R. performed the calculations. J. D. and K. G. wrote the paper. All authors offered constructive comments on the manuscript.

Conflicts of interest

There are no conflicts to declare.

Acknowledgements

We are thankful for the financial support of the National Natural Science Foundation of China (22171135), the Innovative Research Team Program by the Ministry of Education of China (IRT-17R54), the National Natural Science Foundation of Jiangsu Province (BK20231269), the State Key Laboratory of Materials-Oriented Chemical Engineering (SKL-MCE-23A18) and the Education Department of Henan Province (22A150050 and 2023GGJS131).

Notes and references

1 D. S. Sholl and R. P. Lively, *Nature*, 2016, **532**, 435–437.
2 Y. Wang, N. Y. Huang, X. W. Zhang, H. He, R. K. Huang, Z. M. Ye, Y. Li, D. D. Zhou, P. Q. Liao, X. M. Chen and J. P. Zhang, *Angew. Chem., Int. Ed.*, 2019, **58**, 7692–7696.
3 F. A. Da Silva and A. E. Rodrigues, *AIChE J.*, 2001, **47**, 341–357.
4 B. Y. Li, Z. J. Zhang, Y. Li, K. X. Yao, Y. H. Zhu, Z. Y. Deng, F. Yang, X. J. Zhou, G. H. Li, H. H. Wu, N. Nijem, Y. J. Chabal, Z. P. Lai, Y. Han, Z. Shi, S. H. Feng and J. Li, *Angew. Chem., Int. Ed.*, 2012, **51**, 1412–1415.
5 G. K. H. Shimizu, J. M. Taylor and S. Kim, *Science*, 2013, **341**, 354–355.
6 K. S. Walton, *Nat. Chem.*, 2014, **6**, 277–278.
7 S. H. Yang, A. J. Ramirez-Cuesta, R. Newby, V. Garcia-Sakai, P. Manuel, S. K. Callear, S. I. Campbell, C. C. Tang and M. Schroder, *Nat. Chem.*, 2015, **7**, 121–129.
8 T. M. McDonald, J. A. Mason, X. Q. Kong, E. D. Bloch, D. Gygi, A. Dani, V. Crocella, F. Giordanino, S. O. Odoh, W. S. Drisdell, B. Vlaisavljevich, A. L. Dzubak, R. Poloni, S. K. Schnell, N. Planas, K. Lee, T. Pascal, L. W. F. Wan, D. Prendergast, J. B. Neaton, B. Smit, J. B. Kortright, L. Gagliardi, S. Bordiga, J. A. Reimer and J. R. Long, *Nature*, 2015, **519**, 303–308.
9 X. L. Cui, K. J. Chen, H. B. Xing, Q. W. Yang, R. Krishna, Z. B. Bao, H. Wu, W. Zhou, X. L. Dong, Y. Han, B. Li, Q. L. Ren, M. J. Zaworotko and B. L. Chen, *Science*, 2016, **353**, 141–144.
10 S. Krause, V. Bon, I. Senkovska, U. Stoeck, D. Wallacher, D. M. Tobbens, S. Zander, R. S. Pillai, G. Maurin, F. X. Coudert and S. Kaskel, *Nature*, 2016, **532**, 348–352.
11 A. Cadiau, Y. Belmabkhout, K. Adil, P. M. Bhatt, R. S. Pillai, A. Shkurenko, C. Martineau-Corcos, G. Maurin and M. Eddaoudi, *Science*, 2017, **356**, 731–735.
12 P.-Q. Liao, N.-Y. Huang, W.-X. Zhang, J.-P. Zhang and X.-M. Chen, *Science*, 2017, **356**, 1193–1196.

13 H. Furukawa, K. E. Cordova, M. O'Keeffe and O. M. Yaghi, *Science*, 2013, **341**, 1230444–1230455.
14 A. Cadiau, K. Adil, P. M. Bhatt, Y. Belmabkhout and M. Eddaoudi, *Science*, 2016, **353**, 137–140.
15 J. E. Bachman, M. T. Kapelewski, D. A. Reed, M. I. Gonzalez and J. R. Long, *J. Am. Chem. Soc.*, 2017, **139**, 15363–15370.
16 L. Yang, X. Cui, Q. Yang, S. Qian, H. Wu, Z. Bao, Z. Zhang, Q. Ren, W. Zhou, B. Chen and H. Xing, *Adv. Mater.*, 2018, **30**, 1705374.
17 M.-H. Yu, B. Space, D. Franz, W. Zhou, C. He, L. Li, R. Krishna, Z. Chang, W. Li, T.-L. Hu and X.-H. Bu, *J. Am. Chem. Soc.*, 2019, **141**, 17703–17712.
18 T. Ke, Q. Wang, J. Shen, J. Zhou, Z. Bao, Q. Yang and Q. Ren, *Angew. Chem., Int. Ed.*, 2020, **59**, 12725–12730.
19 H. Zeng, M. Xie, T. Wang, R.-J. Wei, X.-J. Xie, Y. Zhao, W. Lu and D. Li, *Nature*, 2021, **595**, 542–548.
20 Q. Dong, Y. Huang, J. Wan, Z. Lu, Z. Wang, C. Gu, J. Duan and J. Bai, *J. Am. Chem. Soc.*, 2023, **145**, 8043–8051.
21 H. Wang, X. L. Dong, V. Colombo, Q. N. Wang, Y. Y. Liu, W. Liu, X. L. Wang, X. Y. Huang, D. M. Proserpio, A. Sironi, Y. Han and J. Li, *Adv. Mater.*, 2018, **30**, 1805088–1805096.
22 D. Antypov, A. Shkurenko, P. M. Bhatt, Y. Belmabkhout, K. Adil, A. Cadiau, M. Suyetin, M. Eddaoudi, M. J. Rosseinsky and M. S. Dyer, *Nat. Commun.*, 2020, **11**, 6099.
23 X. Li, J. Liu, K. Zhou, S. Ullah, H. Wang, J. Zou, T. Thonhauser and J. Li, *J. Am. Chem. Soc.*, 2022, **144**, 21702–21709.
24 K. J. Chen, D. G. Madden, S. Mukherjee, T. Pham, K. A. Forrest, A. Kumar, B. Space, J. Kong, Q. Y. Zhang and M. J. Zaworotko, *Science*, 2019, **366**, 241–246.
25 R. Kitaura, K. Seki, G. Akiyama and S. Kitagawa, *Angew. Chem., Int. Ed.*, 2003, **42**, 428–431.
26 S. Kitagawa and M. Kondo, *Bull. Chem. Soc. Jpn.*, 1998, **71**, 1739–1753.
27 S. Horike, S. Shimomura and S. Kitagawa, *Nat. Chem.*, 2009, **1**, 695–704.
28 N. Behera, J. Duan, W. Jin and S. Kitagawa, *EnergyChem*, 2021, **3**, 100067.
29 V. I. Nikolayenko, D. C. Castell, D. Sensharma, M. Shivanna, L. Loots, K. A. Forrest, C. J. Solanilla-Salinas, K. I. Otake, S. Kitagawa, L. J. Barbour, B. Space and M. J. Zaworotko, *Nat. Chem.*, 2023, **15**, 542–549.
30 D. D. Zhou, P. Chen, C. Wang, S. S. Wang, Y. Du, H. Yan, Z. M. Ye, C. T. He, R. K. Huang, Z. W. Mo, N. Y. Huang and J. P. Zhang, *Nat. Mater.*, 2019, **18**, 994–998.
31 L. B. Li, R. B. Lin, R. Krishna, X. Q. Wang, B. Li, H. Wu, J. P. Li, W. Zhou and B. L. Chen, *J. Am. Chem. Soc.*, 2017, **139**, 7733–7736.
32 J. A. Mason, J. Oktawiec, M. K. Taylor, M. R. Hudson, J. Rodriguez, J. E. Bachman, M. I. Gonzalez, A. Cervellino, A. Guagliardi, C. M. Brown, P. L. Llewellyn, N. Masciocchi and J. R. Long, *Nature*, 2015, **527**, 357–361.
33 J. H. Lee, S. Jeoung, Y. G. Chung and H. R. Moon, *Coord. Chem. Rev.*, 2019, **389**, 161–188.
34 M. Bonneau, C. Lavenn, J.-J. Zheng, A. Legrand, T. Ogawa, K. Sugimoto, F.-X. Coudert, R. Reau, S. Sakaki, K.-i. Otake and S. Kitagawa, *Nat. Chem.*, 2022, **14**, 816–822.
35 A. Schneemann, V. Bon, I. Schwedler, I. Senkovska, S. Kaskel and R. A. Fischer, *Chem. Soc. Rev.*, 2014, **43**, 6062–6096.
36 Y. Huang, J. Wan, T. Pan, K. Ge, Y. Guo, J. Duan, J. Bai, W. Jin and S. Kitagawa, *J. Am. Chem. Soc.*, 2023, **145**, 24425–24432.
37 J. Wan, H. L. Zhou, K. Hyeon-Deuk, I. Y. Chang, Y. Huang, R. Krishna and J. Duan, *Angew. Chem., Int. Ed.*, 2023, **62**, e202316792.
38 M. J. Kalmutzki, N. Hanikel and O. M. Yaghi, *Sci. Adv.*, 2018, **4**, eaat9180.
39 A. L. Spek, *J. Appl. Crystallogr.*, 2003, **36**, 7–13.
40 S. Sen, N. Hosono, J. J. Zheng, S. Kusaka, R. Matsuda, S. Sakaki and S. Kitagawa, *J. Am. Chem. Soc.*, 2017, **139**, 18313–18321.
41 C. Gu, N. Hosono, J. J. Zheng, Y. Sato, S. Kusaka, S. Sakaki and S. Kitagawa, *Science*, 2019, **363**, 387–391.
42 Q. Dong, X. Zhang, S. Liu, R. B. Lin, Y. Guo, Y. Ma, A. Yonezu, R. Krishna, G. Liu, J. Duan, R. Matsuda, W. Jin and B. Chen, *Angew Chem. Int. Ed. Engl.*, 2020, **59**, 22756–22762.
43 C. Kang, Z. Zhang, S. Kusaka, K. Negita, A. K. Usadi, D. C. Calabro, L. S. Baugh, Y. Wang, X. Zou, Z. Huang, R. Matsuda and D. Zhao, *Nat. Mater.*, 2023, **22**, 636–643.
44 J. J. Zheng, S. Kusaka, R. Matsuda, S. Kitagawa and S. Sakaki, *J. Am. Chem. Soc.*, 2018, **140**, 13958–13969.
45 T. Ke, Q. J. Wang, J. Shen, J. Y. Zhou, Z. B. Bao, Q. W. Yang and Q. L. Ren, *Angew. Chem., Int. Ed.*, 2020, **59**, 12725–12730.
46 F. Zheng, R. Chen, Y. Liu, Q. Yang, Z. Zhang, Y. Yang, Q. Ren and Z. Bao, *Adv. Sci.*, 2023, **10**, 2207127.
47 E. D. Bloch, W. L. Queen, R. Krishna, J. M. Zadrozny, C. M. Brown and J. R. Long, *Science*, 2012, **335**, 1606–1610.
48 R. Krishna, *ACS Omega*, 2020, **5**, 16987–17004.